American Mineralogist, Volume 77, pages 987–1003, 1992

Equilibria among Fe-Ti oxides, pyroxenes, olivine, and quartz: Part I. Theory

Donald H. Lindsley
Center for High-Pressure Research, Department of Earth and Space Sciences, State University of New York, Stony Brook, New York 11794, U.S.A.

B. Ronald Frost
Department of Geology and Geophysics, University of Wyoming, Laramie, Wyoming 82071, U.S.A.

Abstract

The Ca-QUIIF system involves 59 equilibria (13 of which are independent) among augite, pigeonite, orthopyroxene, olivine, quartz, titaniferous magnetite, and ilmenite in the system Fe-O-CaO-MgO-SiO_2-TiO_2. Because each of these phases except quartz is a solid solution, most assemblages are more tightly constrained than appears on the basis of their formal, phase-rule variance. For example, five-phase assemblages (and in favorable cases, four-phase assemblages) completely fix the temperature, pressure, f_{O_2}, and silica activity at which they equilibrated. In many cases it is possible to use the constraints of calcium pyroxene QUIIF to recover the original composition of a phase—for example, oxyexsolved titaniferous magnetite—that has reequilibrated during cooling. Even when quantitative recovery of compositions is not possible, calcium pyroxene QUIIF equilibria usually provide tighter constraints on intensive parameters than can be obtained by applying pyroxene-olivine-quartz and two-oxide systems separately.

Introduction and previous work

The concept of interaction between oxides and ferromagnesian silicates dates to 1935, when Bowen and Schairer pointed out that magmas differentiating under relatively reduced conditions would tend to retain Fe in the ferrous state and thus undergo Fe enrichment, whereas those crystallizing under more oxidizing conditions would form early, abundant magnetite, leading to silica enrichment in the residual magma. Perhaps the first worker to apply this idea to specific rock types was Osborn (1959), who suggested that different redox environments might explain the difference between tholeiitic and calc-alkalic rocks. In two papers that set a standard for future studies, Carmichael, using the then newly developed electron microprobe, investigated the relations between Fe-Ti oxides and ferromagnesian silicates for salic volcanic rocks (1967a, 1967b). He found consistent correlations between types of silicates and the f_{O_2}, as indicated by the Fe-Ti oxides.

More recently, the development of thermodynamic solution models for the appropriate mineral groups has permitted the relations discussed by these earlier workers to be calculated quantitatively. Frost et al. (1988) pointed out that f_{O_2} in rocks is reflected not only in the composition of the Fe-Ti oxides, but also in the composition of the coexisting ferromagnesian silicates. The equilibrium

$$\underset{\text{quartz}}{SiO_2} + 2\underset{\text{ulvöspinel}}{Fe_2TiO_4} = 2\underset{\text{ilmenite}}{FeTiO_3} + \underset{\text{fayalite}}{Fe_2SiO_4} \qquad (1)$$

abbreviated QUIIF, governs the composition of the Fe-Ti oxides coexisting with Fe-rich olivine and quartz (Frost et al., 1988). One reason for the importance for the QUIIF equilibrium is that it can reduce the uncertainty inherent in the magnetite-ilmenite thermometer by an order of magnitude; it also allows the petrologist to "see through" much of the reequilibration that commonly affects Fe-Ti oxides in plutonic rocks.

Recently the QUIIF equilibrium has been extended to more magnesian compositions in which Opx becomes stable (Lindsley et al., 1990; Ghiorso and Sack, 1991). Fayalite + quartz are topologically equivalent to Opx; thus in Mg-bearing systems there occurs a whole series of oxide-silicate equilibria relating the composition of Fe-Ti oxides to that of Opx, in either quartz-saturated or olivine-saturated systems.

Calcium pyroxene QUIIF

Lindsley et al. (1990) calibrated these equilibria for the Ca-free system. In this paper we extend this calibration to QUIIF-like equilibria for systems containing Ca-rich pyroxene. Plans for the present paper were laid beginning around 1985, and several features of the solution models were set by information available at that time. No published thermodynamic data base in 1985 contained data for all the end-member phases (four orthopyroxenes, four clinopyroxenes, four olivines, four spinels, three rhombohedral oxides, and quartz) in the calcium pyroxene QUIIF system, so we had to adopt one data base and enlarge it to meet our needs. We chose the data base of Helgeson et al. (1978) but have modified it extensively. Among those modifications are (1) addition of compressibilities and thermal expansivities, (2) adjustment of the free energy of forsterite so that the assemblage forsterite

0003–004X/92/0910–0987$02.00

+ quartz remains metastable up to and above the incongruent melting point of enstatite, (3) adoption of the fayalite data of Robie et al. (1982), and (4) revision of the apparent free energy of ferrosilite to fit the experiments of Bohlen et al. (1980). Because the simultaneous fitting of experimental data for coexisting orthopyroxenes, clinopyroxenes, olivines, and quartz places extremely tight limits on the differences among the apparent free energies of the end-members, once a few end-member values have been adopted, the others can (and must) be constrained by those differences (Fig. 1 of Davidson and Lindsley, 1989). These modifications to the data base of Helgeson et al. are documented in Davidson and Lindsley (1989).

Another important decision was to adopt the compilation of John Haas for O_2 buffers in the system Fe-O-SiO_2, which at the time was the only compilation that had constrained all those buffers to be internally consistent. To our knowledge, this work, which was available to us in draft form, has not yet been published. In accordance with U.S. Geological Survey policy, Haas requested that we cite this work as "personal communication" rather than as an unpublished manuscript. (We provide this information for the reassurance of our colleagues who have asked why we based such an important part of our models on something so insubstantial-sounding as a personal communication.) In our modeling of the oxides (Andersen and Lindsley, 1988; Andersen et al., 1991) and in the QUILF computer program (Andersen et al., in preparation), we use the full expressions of the buffers. However, for ease in routine calculation, Frost et al. (1988) also fitted Haas's data for QIF, FMQ, FHQ, and MH to the familiar $A/T + B + C(P - 1)/T$ form (their Table 1, p. 729). Within the stated temperature ranges, those expressions reproduce the Haas values closely, the worst deviation being 0.06 log units. When the oxide models were merged with the silicate model of Davidson and Lindsley (1989) to produce the calcium pyroxene QUIlF program, the standard-state apparent free energies for the silicates had to be adjusted slightly (but always preserving the all-important differences) so as to be compatible with the Haas buffer data.

Our QUILF program uses two expressions for quartz. For fitting the fayalite + quartz = ferrosilite experiments of Bohlen et al. (1980), we used Equation 111 of Helgeson et al. (1978). (The equation as published contains several errors and has been corrected to conform with SUPCRT computer code of Helgeson and coworkers.) Thus all (nonredox) equilibria involving olivine, pyroxene, and quartz use this expression. When we later adopted the buffer expressions of Haas, on the other hand, it was necessary to use his quartz data for redox equilibria. Hindsight would suggest that we should have refitted Haas's f_{O_2} data so as to use the (modified) Helgeson parameters, but we did not do so. This is unfortunate, but careful bookkeeping—that is, the Haas terms are used only for calculating f_{O_2}, the Helgeson parameters for all other terms—prevents it from being a problem. Agreement between silica activities calculated from silicates only and from oxide-silicate equilibria shows that this approach does not introduce problems.

Readers should note that it is absolutely imperative for the activity-composition models to be mutually consistent. Our oxide and ferromagnesian silicate models are tied together through the use of the same solution model for olivine (Davidson and Mukhopadhyay, 1984). It would be a serious error to modify any of the solution parameters (or substitute another model) without remodeling all the solid solutions so as to be internally consistent. Likewise, no O_2 buffer or end-member standard state should be modified unless one can be certain that all differences in standard-state data remain unchanged. This is not to say that we consider the adopted solution models, buffers, and standard-state data to be uniquely "correct"; in retrospect we might wish we had adopted some other values, but the need for internal consistency is paramount. Thus, even if a reader decided, for example, that the oxide model of Ghiorso and Sack (1989, 1991) is superior to that of Andersen et al. (1991), which we used, it would be a serious mistake to try to combine the Ghiorso-Sack oxide model with the calcium magnesium iron silicate model of Davidson and Lindsley (1989) to produce an "improved" version of calcium pyroxene QUIlF. This is because the Ghiorso-Sack oxide model is consistent with an olivine model that is approximately three times more nonideal than that of Davidson and Mukhopadhyay (1984), and there is no way short of remodeling three ternary systems (calcium magnesium iron olivines, clinopyroxenes, and orthopyroxenes) that the models can be made mutually consistent. We are not claiming that one olivine model is right and the other wrong, only that internal consistency is more important than the details of either model! Thus we encourage readers to apply the internally consistent Opx QUIlF model of Ghiorso and Sack (1991) as well as our own to Ca-free assemblages and to compare the results; at present, however, ours is the only system that quantitatively treats calcium pyroxenes and olivines together with two oxides and quartz.

Equilibria within subsystems of calcium pyroxene QUIlF

Calcium pyroxene QUIlF equilibria occur in a portion of the system Fe-O-MgO-CaO-TiO_2-SiO_2. Simple application of the phase rule to this six-component system shows that eight phases would form an invariant assemblage in which all intensive variables are fixed. We consider at most seven phases in this system: olivine, quartz, three pyroxenes, and two oxides. Although in a phase-rule sense these seven phases would be univariant, this assemblage is exceedingly rare. It has seven possible variables, for example P, T, f_{O_2}, a_{SiO_2}, and three compositional variables, which we can designate $\mu MgFe_{-1}$, $\mu Fe^{2+}TiFe^{3+}_{-2}$, and $\mu Ca(Mg,Fe)_{-1}$, all but one of which would be fixed from phase-rule considerations. But because six of the seven phases are solid solutions, their coexistence further requires that $\mu MgFe_{-1}$ be equal in six phases, that $\mu Fe^{2+}TiFe^{3+}_{-2}$ be equal in the two oxides, and

that $\mu Ca(Mg,Fe)_{-1}$ be equal in the four ferromagnesian silicates. Thus the seven-phase assemblage would be highly overdetermined, and its existence, although plausible based on simple phase-rule variance, would require a very limited range of bulk composition. If such an assemblage were found, with all phases in equilibrium, we would immediately know that the temperature had been 818 ± 10 °C; knowing the Fe/Mg ratio of just one of the phases would also permit calculation of pressure and f_{O_2}—and the compositions of all the other phases. Putting it another way, all the variables can be fixed by as few as four phases, although five phases generally provide a more robust or reliable solution. This paper describes how those variables can be determined. A companion paper (Frost and Lindsley, 1992) illustrates the application of calcium QUIIF to numerous natural occurrences.

The power of calcium pyroxene QUIIF lies in the fact that all phases but quartz are solid solutions; by analyzing them with the electron microprobe and applying appropriate solution models, we can determine the end-member chemical potentials. The total number of reactions and equilibria is large, and the relations among them complex. Under the reasonable (but not perfect) assumption that Fe_2O_3 and TiO_2 are unimportant in the silicates and CaO is absent from the oxides, the independent equilibria include six net-transfer reactions, four Fe-Mg exchange equilibria, two independent Ca-(Fe,Mg) exchanges, and the $Fe^{3+}_{-2}Fe^{2+}Ti^{4+}$ exchange, for a total of 13 independent equilibria. The remaining equilibria can be derived from these 13 but can nevertheless be very useful in special circumstances. In this paper, we use the mineral abbreviations listed in Table 1; Table 2 lists the reactions and equilibria that we have identified and calibrated. The abbreviations in the left column of Table 2 are those used in our computer program QUILF (Andersen et al., in preparation) to calculate equilibria among the various phases; Reaction 1 is not explicitly included because it is the algebraic sum of twice the exchange equilibrium FeTi ($Fe_3O_4 + FeTiO_3 = Fe_2TiO_4 + Fe_2O_3$), the fayalite + magnetite + quartz buffer (FMQ), and the fayalite + hematite + quartz equilibrium (FHQ) (Table 2). Because relations within the six-component system are so complex, and with apologies to readers for whom the next few paragraphs will be obvious, we have chosen to build up to those equilibria starting with very simple examples. For clarity in the discussion that follows, we assume that the phases all lie within the system Fe-O-CaO-MgO-SiO_2-TiO_2, that all phases are in equilibrium and retain their equilibrium compositions, and that the solution models we apply are perfect. In reality, of course, each of these assumptions must be carefully evaluated and assessed; see our companion paper (Frost and Lindsley, 1992).

Table 1. Mineral abbreviations used in this paper

A, Aug = augite
Cpx = clinopyroxene without distinction as to Ca content
F = fayalite ($X_{Fe} > 0.9$)
Fe^0 = metallic Fe
gk = $MgTiO_3$ component in ilmenite
H = hematite (Ti-free)
hem = Fe_2O_3 component in ilmenite
Il = $ilmenite_{ss}$
il = $FeTiO_3$ component in ilmenite
M = Ti-free magnetite
O, Ol = olivine ($X_{Fe} < 0.9$)
Op, Opx = orthopyroxene*
P, Pig = pigeonite
Px = pyroxene (composition and space group not specified)
Q = quartz
Rut = rutile (used only as a reference state for a_{TiO_2})
Sp = iron magnesium titanium spinel
Ti-Mt = titaniferous magnetite (= magnetite-$ulvöspinel_{ss}$)
U = $ulvöspinel_{ss}$ (Ti-bearing magnetite)

* In the acronyms for phase assemblages, Op immediately followed by A or P indicates Opx saturated with a more calcic pyroxene. Otherwise, Op refers to Ca-free or Ca-poor Opx.

The system FeO-SiO_2

Second in importance only to QUIIF (Reaction 1) in our discussion is the reaction:

$$\underset{\text{fayalite}}{Fe_2SiO_4} + \underset{\text{quartz}}{SiO_2} = \underset{\text{ferrosilite}}{Fe_2Si_2O_6} \qquad (2)$$

(FeOlQOpx in Table 2; Bohlen et al., 1980), which relates olivine and quartz to pyroxene. With two components and three phases, this reaction is univariant and is an excellent barometer if the temperature is known. Addition of MgO and CaO extends it to quadrilateral pyroxenes and olivines; addition of O and TiO_2 relates it to QUIIF. In the examples that follow, addition of a component other than O or silica is by exchange vectors like $MgFe_{-1}$.

FeO-MgO-SiO_2

As MgO is added to the system, both fayalite and ferrosilite gain Mg, the exact amounts being controlled by the exchange equilibrium (FeMgOlOpx; Table 2) between them. At some value of $\mu MgFe_{-1}$, olivine + quartz becomes unstable, reacting to form Opx (reaction MgOlQOpx). With the addition of another component (MgO), the assemblage olivine + quartz + Opx has become divariant in a formal or phase-rule sense, but note that we have also added two more constraints, the equilibria FeMgOlOpx and MgOlQOpx. If either of those were a good thermometer (unfortunately, neither is), our higher variance assemblage would actually constrain the system more effectively than does the Mg-free assemblage. Nevertheless, this illustrates the utility of calcium pyroxene QUIIF: although addition of more components increases the formal variance, it also provides a much greater number of constraints through calibrated reactions and equilibria. Thus assemblages of four, five, or six phases tend to be completely determined or even overdetermined in our six-component system.

CaO-FeO-SiO_2

The addition of small amounts of CaO to the fayalite + quartz + ferrosilite assemblage has effects similar to those of adding small amounts of MgO: Ca is partitioned between olivine and pyroxene by the exchange equilib-

TABLE 2. Reactions and equilibria in Ca-PX QUIIF

Abbreviation	Reaction or equilibrium
Equilibria among Q + Sp + Il + Ol + Px + Fe + rutile	
1. Two oxides	
FeTi	$Fe_3O_4 + FeTiO_3 = Fe_2TiO_4 + Fe_2O_3$
MH	$4Fe_3O_4 + O_2 = 6Fe_2O_3$
FeMgIlSp	$MgFe_2O_4 + FeTiO_3 = Fe_3O_4 + MgTiO_3$
2. Silicate + oxide	
FeMgOlIl	$oFe_2SiO_4 + 2MgTiO_3 = oMg_2SiO_4 + 2FeTiO_3$
FeMgAugIl	$aFe_2Si_2O_6 + 2MgTiO_3 = aMg_2Si_2O_6 + 2FeTiO_3$
FeMgCaAugIl*	$aCaFeSi_2O_6 + MgTiO_3 = aCaMgSi_2O_6 + FeTiO_3$
FeMgPigIl	$pFe_2Si_2O_6 + 2MgTiO_3 = pMg_2Si_2O_6 + 2FeTiO_3$
FeMgOpxIl	$\rho Fe_2Si_2O_6 + 2MgTiO_3 = oMg_2Si_2O_6 + 2FeTiO_3$
FeMgCaOpxIl*	$oCaFeSi_2O_6 + MgTiO_3 = oCaMgSi_2O_6 + FeTiO_3$
FeMgOlSp	$oFe_2SiO_4 + 2MgFe_2O_4 = oMg_2SiO_4 + 2Fe_3O_4$
FeMgOpxSp	$oFe_2Si_2O_6 + 2MgFe_2O_4 = oMg_2Si_2O_6 + 2Fe_3O_4$
FeMgAugSp	$aFe_2Si_2O_6 + 2MgFe_2O_4 = aMg_2Si_2O_6 + 2Fe_3O_4$
FeMgPigSp	$pFe_2Si_2O_6 + 2MgFe_2O_4 = pMg_2Si_2O_6 + 2Fe_3O_4$
3. Olivine + pyroxene	
FeMgOlAug	$oMg_2SiO_4 + aFe_2Si_2O_6 = oFe_2SiO_4 + aMg_2Si_2O_6$
FeCaOlAug	$oFe_2SiO_4 + aCaFeSi_2O_6 = oCaFeSiO_4 + aFe_2Si_2O_6$
FeMgCaOlAug*	$oCaMgSiO_4 + aCaFeSi_2O_6 = oCaFeSiO_4 + aCaMgSi_2O_6$
MgCaOlAug	$oMg_2SiO_4 + aCaMgSi_2O_6 = oCaMgSiO_4 + aMg_2Si_2O_6$
FeMgOlPig	$oMg_2SiO_4 + pFe_2Si_2O_6 = oFe_2SiO_4 + pMg_2Si_2O_6$
FeCaOlPig	$oFe_2SiO_4 + pCaFeSi_2O_6 = oCaFeSiO_4 + pFe_2Si_2O_6$
FeMgCaOlPig*	$oCaMgSiO_4 + pCaFeSi_2O_6 = oCaFeSiO_4 + pCaMgSi_2O_6$
MgCaOlPig	$oMg_2SiO_4 + pCaMgSi_2O_6 = oCaMgSiO_4 + pMg_2Si_2O_6$
FeMgOlOpx	$oMg_2SiO_4 + oFe_2Si_2O_6 = oFe_2SiO_4 + oMg_2Si_2O_6$
FeCaOlOpx	$oFe_2SiO_4 + oCaFeSi_2O_6 = oCaFeSiO_4 + oFe_2Si_2O_6$
FeMgCaOlOpx*	$oCaMgSiO_4 + oCaFeSi_2O_6 = oCaFeSiO_4 + oCaMgSi_2O_6$
MgCaOlOpx	$oMg_2SiO_4 + oCaMgSi_2O_6 = oCaMgSiO_4 + oMg_2Si_2O_6$
4. Two pyroxenes	
FeMgAugPig*	$aFe_2Si_2O_6 + pMg_2Si_2O_6 = aMg_2Si_2O_6 + pFe_2Si_2O_6$
FeMgCaAugPig*	$aCaFeSi_2O_6 + pCaMgSi_2O_6 = aCaMgSi_2O_6 + pCaFeSi_2O_6$
MgCaAugPig*	$aMg_2Si_2O_6 + pCaMgSi_2O_6 = aCaMgSi_2O_6 + pMg_2Si_2O_6$
FeCaAugPig*	$aFe_2Si_2O_6 + pCaFeSi_2O_6 = aCaFeSi_2O_6 + pFe_2Si_2O_6$
FeMgAugOpx*	$oMg_2Si_2O_6 + aFe_2Si_2O_6 = aMg_2Si_2O_6 + oFe_2Si_2O_6$
FeMgCaAugOpx*	$oCaMgSi_2O_6 + aCaFeSi_2O_6 = aCaMgSi_2O_6 + oCaFeSi_2O_6$
MgCaAugOpx*	$oCaMgSi_2O_6 + aMg_2Si_2O_6 = aCaMgSi_2O_6 + oMg_2Si_2O_6$
FeCaAugOpx*	$oCaFeSi_2O_6 + aFe_2Si_2O_6 = aCaFeSi_2O_6 + oFe_2Si_2O_6$
FeMgOpxPig*	$oFe_2Si_2O_6 + pMg_2Si_2O_6 = oMg_2Si_2O_6 + pFe_2Si_2O_6$
FeMgCaOpxPig*	$oCaFeSi_2O_6 + pCaMgSi_2O_6 = oCaMgSi_2O_6 + pCaFeSi_2O_6$
MgCaOpxPig*	$oMg_2Si_2O_6 + pCaMgSi_2O_6 = oCaMgSi_2O_6 + pMg_2Si_2O_6$
FeCaOpxPig*	$oFe_2Si_2O_6 + pCaFeSi_2O_6 = oCaFeSi_2O_6 + pFe_2Si_2O_6$
EnAugPig	$aMg_2Si_2O_6 = pMg_2Si_2O_6$
FsAugPig	$aFe_2Si_2O_6 = pFe_2Si_2O_6$
DiAugPig	$aCaMgSi_2O_6 = pCaMgSi_2O_6$
HdAugPig	$aCaFeSi_2O_6 = pCaFeSi_2O_6$
EnAugOpx	$aMg_2Si_2O_6 = oMg_2Si_2O_6$
FsAugOpx	$aFe_2Si_2O_6 = oFe_2Si_2O_6$
DiAugOpx	$aCaMgSi_2O_6 = oCaMgSi_2O_6$
HdAugOpx	$aCaFeSi_2O_6 = oCaFeSi_2O_6$
EnPigOpx	$pMg_2Si_2O_6 = oMg_2Si_2O_6$
FsPigOpx	$pFe_2Si_2O_6 = oFe_2Si_2O_6$
DiPigOpx	$pCaMgSi_2O_6 = oCaMgSi_2O_6$
HdPigOpx	$pCaFeSi_2O_6 = oCaFeSi_2O_6$
5. Olivine + pyroxene + quartz	
MgOlQAug	$aMg_2Si_2O_6 = oMg_2SiO_4 + SiO_2$
FeOlQAug	$aFe_2Si_2O_6 = oFe_2SiO_4 + SiO_2$
CaMgOlQAug*	$aCaMgSi_2O_6 = oCaMgSiO_4 + SiO_2$
CaFeOlQAug*	$aCaFeSi_2O_6 = oCaFeSiO_4 + SiO_2$
MgOlQPig	$pMg_2Si_2O_6 = oMg_2SiO_4 + SiO_2$
FeOlQPig	$pFe_2Si_2O_6 = oFe_2SiO_4 + SiO_2$
CaMgOlQPig*	$pCaMgSi_2O_6 = oCaMgSiO_4 + SiO_2$
CaFeOlQPig*	$pCaFeSi_2O_6 = oCaFeSiO_4 + SiO_2$
MgOlQOpx	$oMg_2Si_2O_6 = oMg_2SiO_4 + SiO_2$
FeOlQOpx	$oFe_2Si_2O_6 = oFe_2SiO_4 + SiO_2$
CaMgOlQOpx*	$oCaMgSi_2O_6 = oCaMgSiO_4 + SiO_2$
CaFeOlQOpx*	$oCaFeSi_2O_6 = oCaFeSiO_4 + SiO_2$
6. Oxide + silicate + quartz	
FMQ	$3oFe_2SiO_4 + O_2 = 2Fe_3O_4 + 3SiO_2$
AMQ	$3aFe_2Si_2O_6 + O_2 = 2Fe_3O_4 + 6SiO_2$
PMQ	$3pFe_2Si_2O_6 + O_2 = 2Fe_3O_4 + 6SiO_2$
OMQ	$3oFe_2Si_2O_6 + O_2 = 2Fe_3O_4 + 6SiO_2$
FHQ	$2oFe_2SiO_4 + O_2 = 2Fe_2O_3 + 2SiO_2$
AHQ	$2aFe_2Si_2O_6 + O_2 = 2Fe_2O_3 + 4SiO_2$
PHQ	$2pFe_2Si_2O_6 + O_2 = 2Fe_2O_3 + 4SiO_2$
OHQ	$2oFe_2Si_2O_6 + O_2 = 2Fe_2O_3 + 4SiO_2$

TABLE 2.—*Continued*

Abbreviation	Equilibria among Q + Sp + Il + Ol + Px + Fe + rutile Reaction or equilibrium
7. Oxide + olivine + pyroxene	
FAM	$6oFe_2SiO_4 + O_2 = 2Fe_3O_4 + 3aFe_2Si_2O_6$
FPM	$6oFe_2SiO_4 + O_2 = 2Fe_3O_4 + 3pFe_2Si_2O_6$
FOM	$6oFe_2SiO_4 + O_2 = 2Fe_3O_4 + 3oFe_2Si_2O_6$
FAH	$4oFe_2SiO_4 + O_2 = 2Fe_2O_3 + 2aFe_2Si_2O_6$
FPH	$4oFe_2SiO_4 + O_2 = 2Fe_2O_3 + 2pFe_2Si_2O_6$
FOH	$4oFe_2SiO_4 + O_2 = 2Fe_2O_3 + 2oFe_2Si_2O_6$
8. Two oxides + silicate + quartz	
DFMQ	$oFe_2SiO_4 + 2Fe_2O_3 = 2Fe_3O_4 + SiO_2$
DAMQ	$aFe_2Si_2O_6 + 2Fe_2O_3 = 2Fe_3O_4 + 2SiO_2$
DPMQ	$pFe_2Si_2O_6 + 2Fe_2O_3 = 2Fe_3O_4 + 2SiO_2$
DOMQ	$oFe_2Si_2O_6 + 2Fe_2O_3 = 2Fe_3O_4 + 2SiO_2$
9. Two oxides + olivine + pyroxene	
DFAM	$2oFe_2SiO_4 + 2Fe_2O_3 = 2Fe_3O_4 + aFe_2Si_2O_6$
DFPM	$2oFe_2SiO_4 + 2Fe_2O_3 = 2Fe_3O_4 + pFe_2Si_2O_6$
DFOM	$2oFe_2SiO_4 + 2Fe_2O_3 = 2Fe_3O_4 + oFe_2Si_2O_6$
10. Two oxides + rutile	
SpIlRut	$TiO_2 + Fe_2TiO_4 = 2FeTiO_3$
11. Two oxides + Fe	
SpIlFe	$2FeTiO_3 + 2Fe + O_2 = 2Fe_2TiO_4$
12. Oxide + Fe + rutile	
IlFeRut	$2Fe + 2TiO_2 + O_2 = 2FeTiO_3$
SpFeRut	$2Fe + TiO_2 + O_2 = Fe_2TiO_4$
13. Silicate + Fe + quartz	
OlFeQtz	$2Fe + SiO_2 + O_2 = oFe_2SiO_4$
AugFeQtz	$2Fe + 2SiO_2 + O_2 = aFe_2Si_2O_6$
PigFeQtz	$2Fe + 2SiO_2 + O_2 = pFe_2Si_2O_6$
OpxFeQtz	$2Fe + 2SiO_2 + O_2 = oFe_2Si_2O_6$

Note: In the abbreviations of the left column, Fe, Mg, Ca, Ti are cations; Ol, Opx, Aug, Pig are calcium magnesium iron olivine, orthopyroxene, augite, and pigeonite, respectively; Sp and Il are iron magnesium titanium spinel (titaniferous magnetite) and ilmenite. In redox and displaced (D) equilibria, F is fayalite end-member; O, P, and A refer to the $Fe_2Si_2O_6$ component in Opx, pigeonite, and augite, respectively. Q and Rut are quartz and rutile or the equivalent components; M and H refer to Fe_3O_4 and Fe_2O_3 components in spinel and ilmenite, respectively. En, Fs, Di, and Hd are the pyroxene end-members $Mg_2Si_2O_6$, $Fe_2Si_2O_6$, $CaMgSi_2O_6$, and $CaFeSi_2O_6$. Fe is metallic Fe or its component. In the formulas, prefix o for an olivine formula (M_2SiO_4) indicates olivine; prefixes o, a, p before pyroxene end-member formulas indicate that component in Opx, augite, or pigeonite, respectively. Fe_2O_3, $FeTiO_3$, and $MgTiO_3$ are components of ilmenite; Fe_3O_4, Fe_2TiO_4, and $MgFe_2O_4$ are components of spinel (titaniferous magnetite).

* These 23 reactions or equilibria are redundant and thus ignored by the program; they are listed here for completeness.

rium FeCaOlOpx. But because the solubility of Ca is limited in both fayalite and ferrosilite, further addition of CaO leads to the formation of a new phase—hedenbergite. This four-phase assemblage is univariant in the phase-rule sense, but now the system is actually overdetermined, for the solubilities of Ca components in Opx and olivine that are in equilibrium with hedenbergite and the $Fe_2Si_2O_6$ content of hedenbergite in equilibrium with either Opx or olivine + quartz are all thermometers (equilibria FsAugOpx, HdAugOpx, and FeCaOlAug combined with CaFeOlQAug; Table 2). Thus the assemblage hedenbergite + ferrosilite + fayalite + quartz is a simultaneous geothermometer and barometer. Unfortunately from the petrologist's viewpoint, however, the Mg-free assemblage is very rare.

FeO-Fe_2O_3-SiO_2 and CaO-FeO-Fe_2O_3-SiO_2

Now suppose that we had added O (or Fe_2O_3) instead of MgO or CaO to the fayalite + quartz + ferrosilite assemblage. As f_{O_2} increases, fayalite begins to oxidize (reaction FMQ), and magnetite joins the assemblage. (Note that we also have another reaction, OMQ, but it does not provide an additional constraint because it is the sum of FMQ and FeOlQOpx.) The new four-phase assemblage is still univariant, so now it would define f_{O_2} as well as pressure if temperature were known. One way to fix temperature would be by the addition of CaO, for the appearance of hedenbergite would provide the three thermometers described above. There would also be a new redox equilibrium (AMQ), but like OMQ it can be derived by the combination of equilibria we have already used and thus is not independent. This five-phase assemblage (which is probably not known in nature) would define pressure, temperature, and f_{O_2}.

CaO-MgO-FeO-Fe_2O_3-SiO_2

Now consider the effect of adding Mg components to the five-phase assemblage in the example above. For low concentrations, Mg would simply partition into the silicates and the magnetite by the exchange equilibria FeMgOlOpx, FeMgOlAug, FeMgOlSp, FeMgOpxSp, and FeMgAugSp, only three of which are independent. The assemblage will continue to define pressure, temperature, and f_{O_2}. Indeed, because Fe-Mg exchange between oxides and silicates is strongly temperature dependent, our system is even more overdetermined than before, despite an increase in phase-rule variance. With further increase in Mg (i.e., increase in $\mu MgFe_{-1}$), either olivine or quartz must disappear as they become mutually incompatible. With the loss of either phase, the formal variance has

increased to three, yet the assemblage still defines pressure, temperature, and f_{O_2}. Furthermore, the quartz-absent assemblage also defines a_{SiO_2} through equilibria such as FMQ and FeOlQOpx. Those same equilibria, plus ones like MgOlQOpx, likewise define the activities of the olivine components in the olivine-absent assemblage. If it seems implausible that a four-phase assemblage can constrain so much, it may help to think sequentially: (1) coexisting pyroxenes fix temperature (with a small uncertainty owing to the unknown pressure); (2) augite + olivine fix a_{SiO_2} (or augite + quartz fix activity of fayalite); (3) quartz + olivine + Opx fix pressure (simply substitute the activity of the missing phase); (4) quartz + olivine + magnetite (again with the appropriate activity substituted) fix f_{O_2}. Finally, we use the calculated pressure to correct the pyroxene temperature and iterate until there are no further changes. (In real life, this assemblage closely constrains only two of the three variables pressure, f_{O_2}, and a_{SiO_2}; to determine all three requires knowing the compositions of the pyroxenes more precisely than can be determined by routine microprobe analysis. Thus it is very helpful if one additional phase is present to constrain one of those parameters. The remaining two would then also be well constrained.) Only the addition of TiO_2 is needed to develop the calcium pyroxene QUIIF system.

FeO-Fe_2O_3-TiO_2 and FeO-MgO-Fe_2O_3-TiO_2

The assemblage of interest in these subsystems is of course ilmenite plus titaniferous magnetite (Sp in Table 2). What makes these minerals special is that each is a solid solution between end-members having different oxidation states. Thus we have FeTi (a coupled exchange equilibrium, $Fe^{2+}Ti^{4+}Fe^{3+}_{-2}$), which is strongly sensitive to temperature and essentially independent of pressure, and MH, an excellent oxybarometer (Buddington and Lindsley, 1964; Andersen and Lindsley, 1988). As Mg is added, it partitions according to equilibrium FeMgIlSp, but it has only minor effects on the calculated temperature and f_{O_2}. The two-phase assemblage in the four-component system has a formal variance of four, yet it tightly constrains two intensive parameters.

FeO-MgO-Fe_2O_3-TiO_2-SiO_2

Now consider what happens when silica is added to the Fe-Ti oxides. If only a small amount is added, it will react with FeO and MgO to make olivine; FeMgOlSp and FeMgOlIl govern the exchange. Equilibria such as FMQ and FHQ fix a_{SiO_2}, inasmuch as f_{O_2} has been defined by the composition of the oxides. As silica increases, quartz forms if the bulk Fe/Mg ratio is high, leading to the QUIIF assemblage (Reaction 1; Frost et al., 1988). If there is sufficient Mg in the system, increasing silica leads first to the formation of Opx, then to the disappearance of olivine, and finally to the appearance of quartz. Assemblages of two oxides with olivine, with olivine + Opx, with Opx, and with Opx and quartz are part of Opx-QUIIF and were discussed in detail by Lindsley et al. (1990; see also Ghiorso and Sack, 1991).

CaO-FeO-MgO-Fe_2O_3-TiO_2-SiO_2

The addition of CaO to the system above completes the calcium pyroxene QUIIF system. For a seven-phase assemblage (three pyroxenes, two oxides, olivine, and quartz), the first 82 equilibria in Table 2 would all apply. However, the 23 equilibria followed by an asterisk in the table are completely redundant and thus are not used in computer program QUILF. Not all the remaining 59 are independent, but all are useful under some circumstances. The eight additional equilibria at the bottom of Table 2 permit the calculation of a_{Fe} and a_{TiO_2} by program QUILF, if the appropriate phases are present.

Topologic relations

Now that some of the principles of calcium pyroxene QUIIF have been laid out, it is useful to consider some phase diagrams. One useful type of diagram is the isothermal, isobaric plot of log f_{O_2} vs. $\mu MgFe_{-1}$. For the reasons given by Frost et al. (1988), we use Δ log f_{O_2} (defined as log f_{O_2} of the sample minus that of the FMQ buffer at the temperature of interest); however, unlike Frost et al., who used 1 bar as the reference state, we follow Lindsley et al. (1990) in using the pressure of interest as the reference because pyroxene-bearing reactions are more pressure sensitive than pyroxene-free reactions. The choice of $\mu MgFe_{-1}$ as the compositional parameter has both good and bad points. Because it is equal in all coexisting phases, it is appropriate for all assemblages. However, its conversion to more conventional components is not intuitive, and it has the further disadvantage that it ranges from $+\infty$ to $-\infty$. Therefore, except for the schematic Figure 1, we compromise and plot the variable X_{Fe}^{Opx} [= $Fe^{2+}/(Fe^{2+} + Mg)$ in Opx] as a monitor for $\mu MgFe_{-1}$. Note that this variable can be expressed even for assemblages that lack Opx simply by calculating the fictive Opx that would be in Fe-Mg exchange equilibrium (but not phase equilibrium) with one of the ferromagnesian phases that is present.

The system Fe-O-MgO-SiO_2-TiO_2

The basic topology for the Ca-free system is that described for Opx, quartz, olivine, and Fe-Ti oxides by Lindsley et al. (1990) and reproduced here as Figure 1. Abbreviations used in this and following figures are derived from Lindsley et al. and are listed in Table 1; these abbreviations differ somewhat from those used in Table 2 and the associated text but are adopted both for consistency with the earlier paper and to keep the acronyms for various assemblages at reasonable lengths. It is also helpful to distinguish between an assemblage (for example, OpUIlO) and the many equilibria (FeTi, MH, FeMgIlSp, FeMgOlIl, FeMgOpxIl, FeMgOlSp, FeMgOpxSp, FeMgOlOpx, FOM, FOH, and DFOM; Table 2) that are possible among the phases of that assemblage.

The upper curves in Figure 1 (MH, OMQ, OMOp, OpMQ, OpHQ) are all degenerate in that they lack Ti-bearing phases; they show the effect of Fe-Mg exchange on equilibria involving pure magnetite or hematite. These

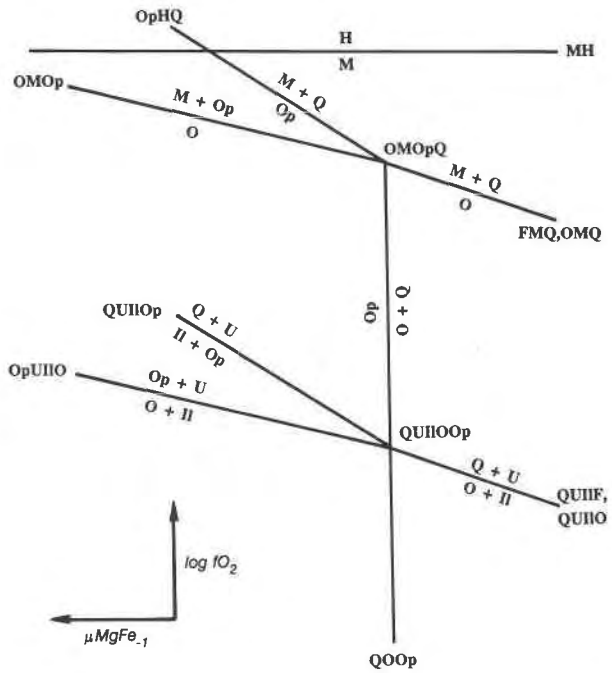

Fig. 1. Schematic diagram of $\mu MgFe_{-1}$ vs. f_{O_2} for the Ca-free system (Lindsley et al., 1990) for arbitrary fixed pressure and temperature. Abbreviations as in Table 1.

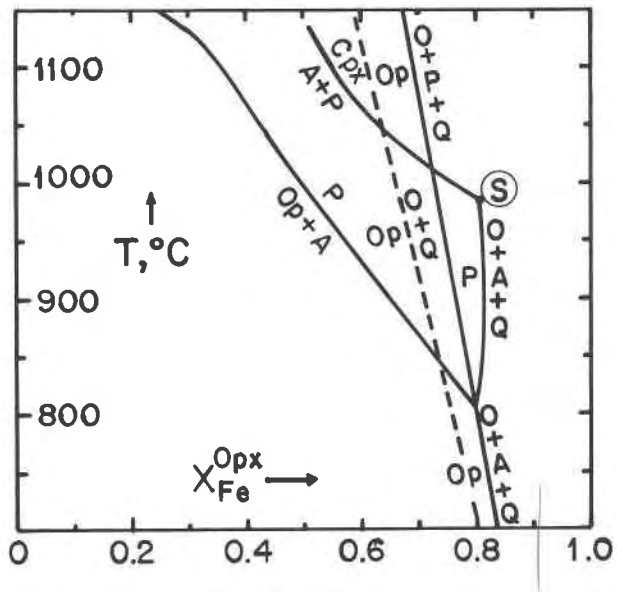

Fig. 2. Diagram of X_{Fe}^{Opx} ($\mu MgFe_{-1}$) vs. T for the system CaO-FeO-MgO-SiO_2, showing isobaric (3-kbar) univariant reactions among pyroxenes, olivine, and quartz.

univariant equilibria become divariant in the Ti-bearing system, with the Ti contents of magnetite and of hematite increasing with decreasing f_{O_2}. At f_{O_2} where the magnetite becomes saturated with Ti and ilmenite becomes stable, the QUIIF-type reactions (QUIIF, QUIIO, QUIIOp, OpUIIO) appear.

As Mg is added to Mg-free compositions (right side of Fig. 1), the FMQ assemblage becomes the assemblage OMQ, which is (isothermally and isobarically) univariant and thus plots as a line. Similarly, with the addition of Mg, QUIIF becomes QUIIO and is also univariant. Because Mg is preferentially accepted in silicates relative to oxides, increasing $\mu MgFe_{-1}$ causes both OMQ and QUIIO to become displaced to higher f_{O_2}. With increasing Mg, each of these curves intersects QOOp at the value of $\mu MgFe_{-1}$ for which olivine and quartz can no longer be in equilibrium. QOOp is vertical in Figure 1 because it is independent of f_{O_2}. The intersections of OMQ and QUIIO with QOOp produce the (isothermally and isobarically) invariant points OMOpQ and QUIIOOp. To the left of each point are two new curves, one quartz-absent (OMOp, OpUIIO) and the other olivine-absent (OpMQ, QUIIOp). These curves are the mainstays of (Ca-free) pyroxene QUIIF. Lindsley et al. (1990, their Fig. 2) show the location of curves for 3 kbar and at 600, 800, 1000, and 1200 °C. The following figures are also for 3 kbar, both to aid comparison with the earlier results and because that pressure is a reasonable approximation for many plutonic rocks and volcanic phenocryst assemblages.

The system Fe-O-CaO-MgO-SiO_2-TiO_2

The addition of Ca increases the variance by one, so the (isobarically and isothermally) univariant curves in Figure 1 become divariant surfaces. Univariance is restored when sufficient Ca has been added that the system becomes saturated with augite (or pigeonite). To aid the reader in visualizing the relations between the Ca-free topologies described by Lindsley et al. (1990) and those for calcium pyroxene QUIIF, we first discuss the subsystem CaO-FeO-MgO-SiO_2.

Subsystem CaO-FeO-MgO-SiO_2. One way to depict the relations between pyroxenes, olivine, and quartz is on an isobaric T-$\mu MgFe_{-1}$ (X_{Fe}^{Opx}) diagram (Fig. 2). Two points are of particular interest on this diagram. One is the (isobarically) invariant point marking the low-temperature limit for the stability of pigeonite, 808 °C at this pressure. The other is the singular point S (977 °C) at which pigeonite and augite (in equilibrium with olivine and quartz) become indistinguishable. Also shown on this figure in dashed lines is the location of the reaction OQOp. This lies at lower X_{Fe}^{Opx} than the corresponding Ca-bearing reactions because the preferential substitution of Ca into Opx relative to olivine will stabilize Opx to lower $\mu MgFe_{-1}$ in the Ca-bearing system. A more traditional way of viewing pyroxene relations is to use an isobaric, isothermal chemographic projection, the familiar pyroxene quadrilateral. Figures 3A, 3C, 3E, and 3G show such projections at 3 kbar and 800, 900, 1000, and 1100 °C. At temperatures below the stability of pigeonite, such as 800 °C (Fig. 3A), there is only one univariant reaction, which is represented by the three-phase triangle labeled (QOOpA in Figure 3A. This reaction is

augite + olivine + quartz = Opx (QOOpA). (3)

Note that Reaction 3 is distinct from the analogous Ca-free reaction

$$\underset{\text{olivine}}{Fe_2SiO_4} + \underset{\text{quartz}}{SiO_2} = \underset{\text{Opx}}{Fe_2Si_2O_6} \quad \text{(QOOp)}$$

because the Opx in Reaction 3 is saturated in Ca. Furthermore, because the Ca content of the Opx is variable, the stoichiometry of Reaction 3 cannot be specified without fixing T and P. Another way to view the distinction is to note that OQOp is equivalent to equilibrium FeOlQOpx, whereas Reaction 3 is the combination of FeOlQOpx, MgOlQOpx, and FeCaOlOpx (Table 2).

At the temperature of the minimum stability of pigeonite (808 °C at 3 kbar), Reaction 3 terminates at an isobaric invariant point (Fig. 2); three other univariant reactions appear at higher temperatures. These are

Opx + augite = pigeonite (OpAP) (4)

Opx = pigeonite + olivine + quartz (QOOpP) (5)

pigeonite = olivine + quartz + augite (QOAP). (6)

Chemographic relationships among these three reactions are shown in Figure 3C for 900 °C. Note in Figure 3C that the consolute point APCpx between pigeonite and augite is metastable with respect to olivine + augite + quartz.

At still higher temperatures (977 °C at 3 kbar) the consolute point between augite and pigeonite becomes stable and migrates toward progressively more magnesian compositions with increasing temperature. The appearance of the consolute point at Fe-rich compositions makes Reaction 6 metastable because at temperatures above the consolute point one cannot distinguish between augite and pigeonite as separate phases. This results in the topology shown in Figures 3E and 3G, for temperatures 1000 and 1100 °C, respectively. In place of Reaction 6 another univariant reaction appears:

augite + pigeonite = one clinopyroxene (APCpx). (7)

Because it is degenerate, Reaction 7 appears on Figures 3E and 3G simply as the consolute point. One result of Reaction 7 is that the assemblage QOA grades continuously into QOP with increasing Mg (Figs. 3E, 3G).

System Fe-O-CaO-MgO-SiO$_2$-TiO$_2$. The topology for the system CaO-FeO-MgO-SiO$_2$ shown in Figure 2 forms the basis for the isothermal, isobaric diagrams of Δ log f_{O_2} vs. X_{Fe}^{Opx} of the system Fe-O-CaO-MgO-SiO$_2$-TiO$_2$ (Figs. 3B, 3D, 3F, 3H). Each reaction of Figure 2 appears as a vertical line, independent of f_{O_2} in Figures 3B, 3D, 3F, and 3H. To avoid constant repetition in the following discussion, we shall not repeat that the diagrams are for constant temperature and pressure. The reader should bear in mind, however, that the terms invariant, univariant, and divariant apply only for isothermal and isobaric conditions. It should also be noted that, although the pyroxene-olivine-quartz models are calibrated for the entire range of these figures, the oxide models are not. For the most part, the oxide models have been calibrated only for values of Δ log f_{O_2} below +2. For purposes of illustration, we have included some equilibria that plot above this range, but the reader should be aware that the calculations become increasingly less precise at higher values of Δ log f_{O_2}.

For temperatures below the stability of pigeonite, such as 800 °C (Fig. 3B), the only difference between the topology for the Ca-free system (i.e., Fig. 1) and that of the calcic system is a slight difference in the stoichiometry of the reactions and hence a slight displacement of the univariant curves. Reactions OMQ, OpMQ, and OMOp of Figure 1 become, respectively,

olivine + O_2 = magnetite + quartz + augite (OMQA) (8)

Opx + O_2 = magnetite + quartz + augite (OpAMQ) (9)

and

olivine + augite + O_2 = Opx + magnetite (OMOpA). (10)

Likewise, in the Ca-saturated system reactions QUIIO, QUIIOp, and OpUIIO (Table 3) become, respectively,

quartz + ulvöspinel + augite = ilmenite + olivine (QUIIOA) (11)

quartz + ulvöspinel + augite = ilmenite + Opx (QUIIOpA) (12)

and

Opx + ulvöspinel = olivine + augite + ilmenite (OpAUIIO). (13)

The solution of Ca into Opx causes an expansion of the Opx field, both to higher X_{Fe} and to higher and lower f_{O_2}, although the change in f_{O_2} is slight (Fig. 3B). Likewise, the limited solution of Ca into olivine causes Reactions 8 and 11 to lie at slightly higher f_{O_2} than their Ca-free counterparts. The curves for the Ca-free system are shown as dashed lines in Figure 3B for comparison at 800 °C; they are omitted for clarity in the diagrams at higher temperatures.

The topologies for higher temperatures are more complex (Figs. 3D, 3F, 3H) because of the presence of pigeonite. The Ca-free reaction OpMQ is replaced by

pigeonite + O_2 = magnetite + quartz + augite (APMQ) (14)

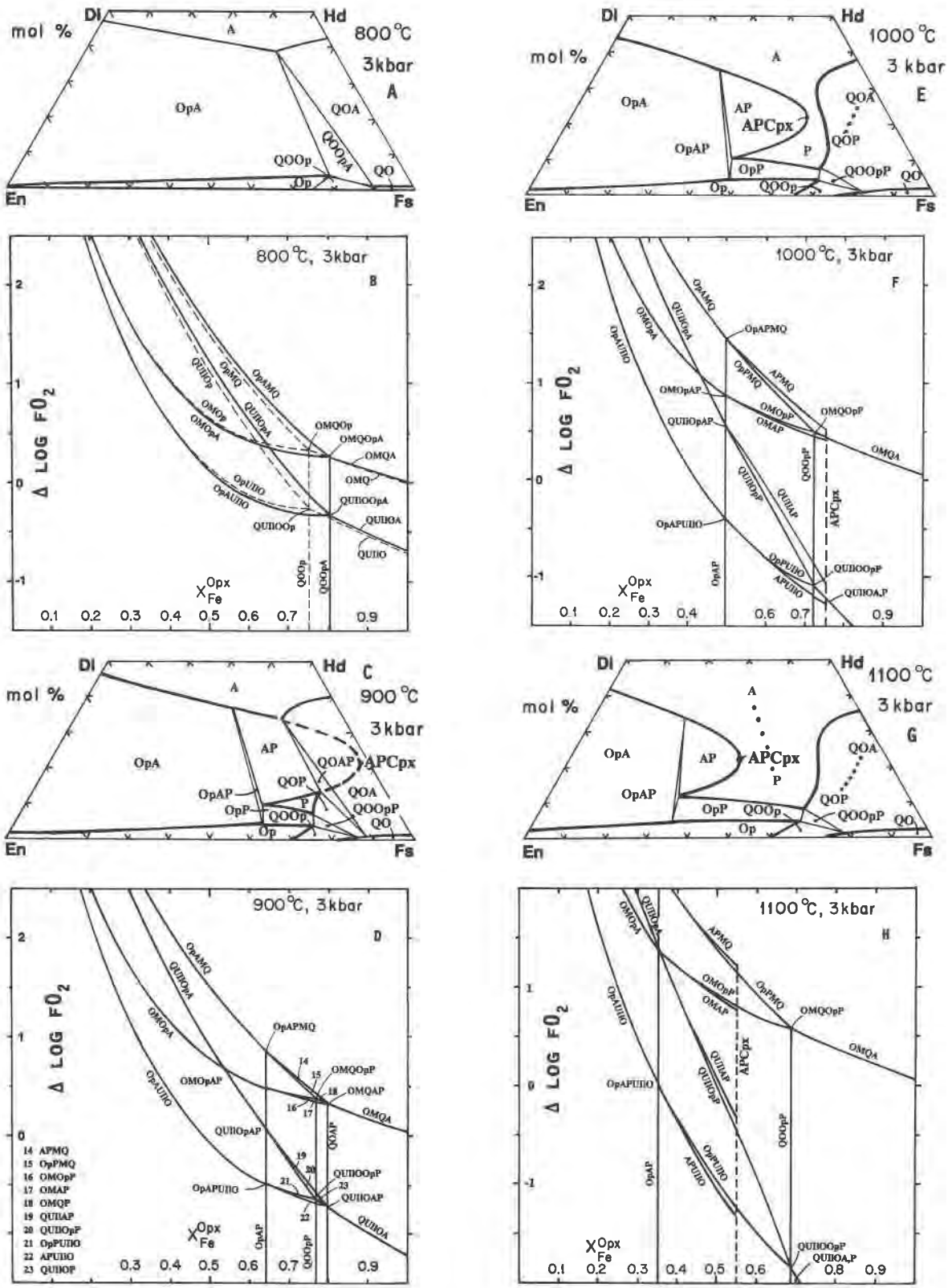

Fig. 3. Isothermal, isobaric pyroxene quadrilateral diagrams and diagrams of X_{Fe}^{Opx} ($\mu MgFe_{-1}$) vs. $\Delta \log f_{O_2}$ (FMQ) for the system Ca-Fe-Mg-Ti-Si-O at 3 kbar: (**A**), (**B**) 800 °C; (**C**), (**D**) 900 °C; (**E**), (**F**) 1000 °C; (**G**), (**H**) 1100 °C. Abbreviations for phases are given in Table 1, and acronyms are keyed to specific reactions in the text. The apparent coincidence of invariant points OMOpAP and QUIIOpAP at 1100 °C (**H**) is simply that: the indifferent crossing of curves QUIIOpA and OMOpA (1000 °C; **F**) just happens to occur at the composition of the OpAP equilibrium at 1100 °C.

TABLE 3. Names and definitions for some input variables used in program QUILF

Variable	Definition
N_{Ti}	number of Ti in spinel (three cations/four O atoms)
N_{Mg}	number of Mg in spinel (three cations/four O atoms)
N_{Mn}	number of Mn in spinel (three cations/four O atoms)
X_{gk}	$MgTiO_3/(Fe_2O_3 + FeTiO_3 + MgTiO_3 + MnTiO_3)$ in ilmenite
X_{hem}	$Fe_2O_3/(Fe_2O_3 + FeTiO_3 + MgTiO_3 + MnTiO_3)$ in ilmenite
X_{il}	$FeTiO_3/(Fe_2O_3 + FeTiO_3 + MgTiO_3 + MnTiO_3)$ in ilmenite
X_{py}	$MnTiO_3/(Fe_2O_3 + FeTiO_3 + MgTiO_3 + MnTiO_3)$ in ilmenite
X_{fo}	Mg/(Mg + Fe + Ca) in olivine
X_{fa}	Ca/(Mg + Fe + Ca) in olivine
X_{En}^{aug}	En/(En + Fs + Wo) in augite
X_{Wo}^{aug}	Wo/(En + Fs + Wo) in augite
X_{En}^{pig}	En/(En + Fs + Wo) in pigeonite
X_{Wo}^{pig}	Wo/(En + Fs + Wo) in pigeonite
X_{En}^{opx}	En/(En + Fs + Wo) in orthopyroxene
X_{Wo}^{opx}	Wo/(En + Fs + Wo) in orthopyroxene
dfmq	log f_{O_2} relative to FMQ buffer at *P*, *T*

Note: Some of the variable names given above differ from commonly used abbreviations. We present these terms to eliminate any ambiguity for readers who may wish to use the QUILF program.

$$\text{Opx} + O_2 = \text{magnetite} + \text{quartz} + \text{pigeonite} \quad \text{(OpPMQ)}. \quad (15)$$

The Ca-free redox reaction OMOp is similarly replaced by

$$\text{pigeonite} + \text{olivine} + O_2 = \text{magnetite} + \text{Opx} \quad \text{(OMOpP)} \quad (16)$$

$$\text{olivine} + \text{augite} + O_2 = \text{magnetite} + \text{pigeonite} \quad \text{(OMAP)} \quad (17)$$

$$\text{olivine} + O_2 = \text{magnetite} + \text{quartz} + \text{pigeonite} \quad \text{(OMQP)}. \quad (18)$$

QUIIOp becomes:

$$\text{quartz} + \text{augite} + \text{ulvöspinel} = \text{pigeonite} + \text{ilmenite} \quad \text{(QUIIAP)} \quad (19)$$

$$\text{quartz} + \text{pigeonite} + \text{ulvöspinel} = \text{Opx} + \text{ilmenite} \quad \text{(QUIIOpP)} \quad (20)$$

and OpUIIO becomes:

$$\text{Opx} + \text{ulvöspinel} = \text{olivine} + \text{pigeonite} + \text{ilmenite} \quad \text{(OpPUIIO)} \quad (21)$$

$$\text{pigeonite} + \text{ulvöspinel} = \text{olivine} + \text{augite} + \text{ilmenite} \quad \text{(APUIIO)} \quad (22)$$

$$\text{quartz} + \text{ulvöspinel} + \text{pigeonite} = \text{ilmenite} + \text{olivine} \quad \text{(QUIIOP)}. \quad (23)$$

At temperatures where Reaction 6 is stable, such as at 900 °C (Fig. 3D), Equilibria 14, 17, 19, and 22 are generated at high X_{Fe} by the intersection of Reaction 6 with Equilibria 8, OMQA, and 11, QUIIOA. At slightly lower X_{Fe}, Reactions 8, OMQA, and 11, QUIIOA, are terminated by intersection with Reaction 4, OpAP, generating Equilibria 15, OpPMQ; 16, OMOpP; 20, QUIIOpP; and 21, OpPUIIO. These pigeonite-bearing reactions (Reactions 15, OpPMQ, through 23, QUIIOP) are terminated at still lower X_{Fe} when they intersect Reaction 4, OpAP. At this point Reactions 9, OpAMQ; 10, OMOpA; 12, QUIIOpA; and 13, OpAUIIO become stable.

With the appearance of pigeonite, the invariant points OMOpAQ and QUIIOOpA (Fig. 3B) each become three points: OpAPMQ, OMAPQ, and OMQOpP; and QUIIOpAP, QUIIOAP, and OpAPUIIO (Fig. 3D). This corresponds directly, of course, to the existence of only one curve at 800 °C, but three curves at 900 °C in Figure 2.

At temperatures (such as 1000 and 1100 °C, Figs. 3F, 3H) above the singularity S in Figure 2, Reactions 14 APMQ; 17, OMAP; 19, QUIIAP; and 22, APUIIO, which involve both pigeonite and augite, are terminated at low X_{Fe} by their intersection with the consolute point of the augite-pigeonite solvus (Reaction 7, APCpx). These intersections are singular points; no corresponding reaction is present on the high X_{Fe} side of them, and they are left awkwardly dangling with only a dashed vertical line (APCpx) for support. Also as a result of Reaction 7, APCpx, becoming stable, assemblage QUIIOA grades continuously into QUIIOP as X_{Fe}^{Opx} decreases (Figs. 3F, 3H); this is directly analogous to the continuous gradation of QOA to QOP (Figs. 3E, 3G).

Figures 3F and 3H appear superficially similar; the topologic difference between them results from the crossover between APCpx and OMQOpP at 1010 °C (Fig. 2) and the consequent reversal of their positions in Figures 3F and 3H.

One important feature to be seen in Figures 3B, 3D, 3F, and 3H is the increased separation in f_{O_2} between the Ti-free and ilmenite-saturated invariant points with increasing temperature. This fact reflects both an increase in $\Delta \log f_{O_2}$ of the Ti-free equilibria with increasing $\mu MgFe_{-1}$ and the strong increase of Ti in the spinel with an attendant decrease in $\Delta \log f_{O_2}$ of QUIIF and its derivative reactions with increasing temperature (Frost et al., 1988). At pressures above 3 kbar, the univariant curves in Figure 2 and the corresponding vertical lines and invariant points in Figure 3 would be displaced to higher values of X_{Fe}^{Opx}, but the general topology would be little changed until pressures are achieved where pure ferrosilite become stable relative to fayalite and quartz.

Compositional variations in the oxides

The five-phase curves such as QUIIOpA and APUIIO in Figures 3B, 3D, 3F, and 3H represent the most useful assemblages for applying calcium pyroxene QUIIF (Frost and Lindsley, 1992), for these assemblages are sufficient to constrain all the relevant intensive parameters. The actual compositions of the phases will be functions of temperature and pressure. Petrologists have been used to

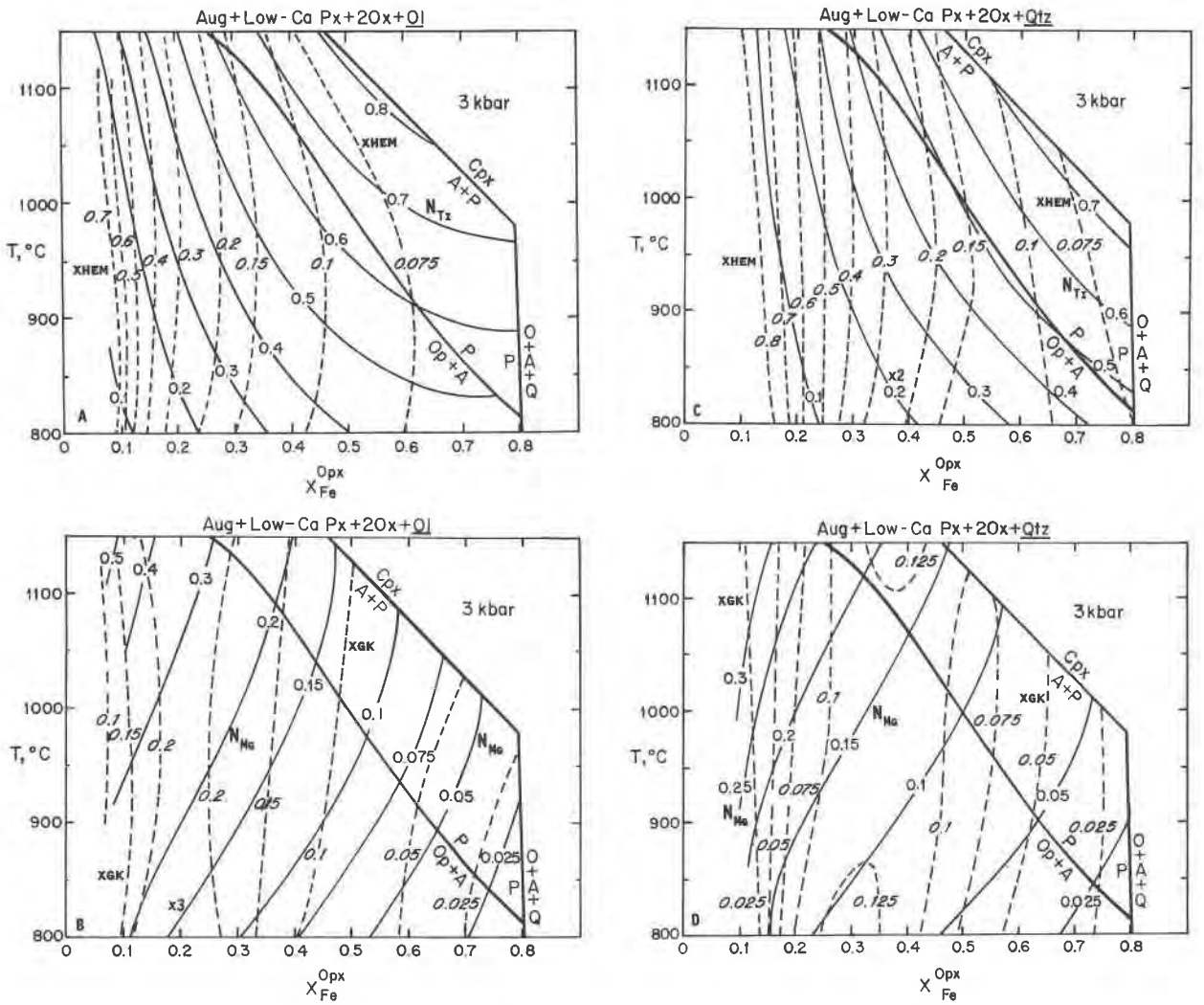

Fig. 4. Plots of T vs. X_{Fe}^{Opx} contouring compositional parameters for selected calcium pyroxene QUIIF equilibria at 3 kbar. The assemblages are for Ca-poor pyroxene (Opx or pigeonite) + augite + 2 oxides with olivine (**A**), (**B**) or with quartz (**C**), (**D**). **A** and **C** give contours for N_{Ti} in spinel (solid lines) and X_{hem} in ilmenite (dashed lines); **B** and **D** show the Mg contours of N_{Mg} in spinel (solid lines) and X_{gk} in ilmenite (dashed lines). Heavy lines show the (isobaric) univariant equilibrium OpAP,which separates subassemblage OpA on the left from AP on the right. The diagrams are terminated on the right by reaction QOAP from 808 to 977 °C and by reaction APCpx above 977 °C (Fig. 2).

considering the oxide minerals as binary oxides, but of course they are more complex. Mg components play an important role in pyroxene QUIIF equilibria, and their variation is important. The variation of oxide compositions with X_{Fe}^{Opx} and temperature at 3 kbar is shown in Figure 4. Figures 4A and 4B are for the assemblages OpAUIIO and APUIIO; Figures 4C and 4D are for the quartz-bearing equivalents QUIIOpA and QUIIAP (the change from Op to P as the low-Ca pyroxene does not seem to affect the curves, so both sets of assemblages are shown. It is important when viewing these diagrams to keep the topology of Figure 3 in mind: the plots for these assemblages curve toward higher f_{O_2} with decreasing X_{Fe}^{Opx}.

In the solution models, ilmenite is treated as a three-component solution with the component $FeTiO_3$ (ilm), Fe_2O_3 (hem), and $MgTiO_3$ (gk) (Andersen and Lindsley, 1988; Andersen et al., 1991), so the ilmenite compositions in Figure 4 are simply the mole fractions x_{hem} and x_{gk}. The spinels are somewhat more complicated; although there are four spinel end-members (Fe_3O_4, $MgFe_2O_4$, Fe_2TiO_4, and Mg_2TiO_4), the assumptions of the model result in only two independent compositional parameters: N_{Ti} (the number of Ti in one formula unit of four-O atoms) and N_{Mg} (the number of Mg atoms per formula unit), and these are contoured. Note that N_{Mg} varies from zero to one for Ti-free spinels but can range up to two for the Fe^{3+}-free join. These compositional pa-

TABLE 4. Calcium pyroxene QUIIF assemblages and information they provide

Assemblage	Information
Assemblages that are overdetermined*	
QUIIOOpAP	T = 818 ± 10 °C; P, f_{O_2} if Fe/Mg is known for one phase
QIIOOpAP	T = 818 ± 10 °C; P, f_{O_2} if Fe/Mg is known for two phases
QUOOpAP	T = 818 ± 10 °C; P, f_{O_2} if Fe/Mg is known for two phases
QUIIOOpA QUIIOOpP QUIIOAP QUIIOpAP	T, P, f_{O_2}; need comp. of two phases
OpAPUIIO	T, P, f_{O_2}, a_{SiO_2}; need comp. of three phases
QUIIOOp QUIIOA QUIIOP QIIOOpA QIIOOpP QIIOAP QUOOpA QUOOpP QUOAP	T, P, f_{O_2}; need comp. of three phases
OpAUIIO OpPUIIO APUIIO OpAPUII	T, P, f_{O_2}, a_{SiO_2}; need comp. of four phases
Assemblages that are fully determined**	
All four-phase assemblages:	
With quartz	T, P, f_{O_2}; need comp. of three phases
Without quartz	T, P, f_{O_2}, a_{SiO_2}; need comp. of four phases
Assemblages that are not fully determined (examples only)	
UII	T, f_{O_2}
UII + O or Px	T, f_{O_2}; a_{SiO_2} if P is known, or vice versa
2 Px + O	T; a_{SiO_2} if P is known, or vice versa
2 Px + U or II	T; any two of P, f_{O_2}, a_{SiO_2} if the third is known
UO + Px	f_{O_2}, a_{SiO_2} if P, T are known

Note: Quartz is assumed to be pure; compositions required to be known are for the remaining phases. Abbreviations as in Table 1.

* Conditions can be estimated even if one phase has undergone extensive reequilibration.

** However, for some assemblages, it may be necessary to know compositions more accurately than can be obtained by routine microprobe analysis. For these, it will be useful to have an independent estimate of P, f_{O_2}, or a_{SiO_2}.

rameters are summarized in Table 3. Once again, the reader should bear in mind that the oxide models were calibrated below $\Delta \log f_{O_2} = +2$, which corresponds approximately to $x_{hem} = 0.3$ in the ilmenite. Thus the compositions become increasingly less reliable in the Mg-rich portions of Figure 4. We include those compositions for purposes of illustration, because the patterns should be correct even if the details are not.

Several features stand out in Figure 4. Note that for any given X_{Fe}^{Opx} and T, N_{Ti} is always higher for the olivine-saturated assemblages than for the quartz-saturated ones. This is because the latter fall at higher values of $\Delta \log f_{O_2}$. Over much of the range of the diagrams, x_{hem} and x_{gk} are almost independent of temperature and are mainly functions of X_{Fe}^{Opx} (Figs. 4B, 4D); recall, however, that f_{O_2} also changes with X_{Fe}^{Opx} (Fig. 3). Note also that x_{gk} goes through a maximum near $X_{Fe}^{Opx} = 0.2$ (olivine-saturated) and $X_{Fe}^{Opx} = 0.35$ (quartz-saturated); for more magnesian Opx, x_{gk} appears to decrease. It might be tempting to ascribe these results to the lower reliability of the oxide models for higher values of f_{O_2} (note that x_{hem} approaches the limit of calibration near the maxima), but we suspect the maxima are real. The x_{gk} decreases with increasing X_{Fe}^{Opx} only because x_{hem} increases even faster, thus greatly lowering both x_{gk} and x_{il}. The ratio $x_{gk}/(x_{gk} + x_{il})$ continues to increase. No such maximum is seen in N_{Mg}, the analogous Mg component in titaniferous magnetite, probably because the Fe_3O_4 content of the spinel does not change as dramatically as does Fe_2O_3 in ilmenite. N_{Mg} is strongly dependent on temperature, showing that Fe-Mg exchange between spinel and the silicates is potentially a good thermometer.

Another interesting point evident from Figure 4 is that titaniferous magnetite accommodates large amounts of Mg ($N_{Mg} > 0.3$) only when in equilibrium with very Mg-rich silicates. Such conditions will be highly oxidizing, and the coexisting rhombic phase will be rich in hematite. Both because the oxides will tend to be nonstoichiometric and because our solution models are not calibrated for such conditions, it is impossible to apply Figure 4 quantitatively to rocks with magnesioferrite-rich spinels, but qualitatively the relations shown on Figure 4 fit with those observed in an oxidized alkali gabbro from Hawaii (Johnston and Stout, 1984), where Mg-rich magnetite occurs with titaniferous hematite and very magnesian Opx (En_{94}).

One possible use of Figures 4A–4D would be to make a quick estimate as to whether the phases of an assemblage could be in equilibrium. Such a procedure is probably valid as a first approximation for N_{Ti} and X_{hem}. However, it appears likely that many oxides, even those in rapidly cooled volcanic rocks, reset their Mg contents by exchange with their surroundings (Frost and Lindsley, 1992), so that disagreement between N_{Ti} or X_{gk} and X_{Fe}^{Opx} need not necessarily indicate that an assemblage is unsuitable for applying calcium pyroxene QUIIF.

Constraints provided by calcium pyroxene QUIIF

The reader who has reached this point is probably wearily wondering, what all this is good for. Table 4 summarizes the types of information that can be obtained from a variety of calcium pyroxene QUIIF assemblages, as well as any additional data that may be needed. It should be apparent that many of these assemblages occur in a very wide variety of igneous rocks, and thus equilibria described in this paper should be widely applicable. For brevity, only a few examples of under-determined assemblages are listed in Table 4.

Use of calcium pyroxene QUIIF to constrain intensive parameters

Numerous examples of applying calcium pyroxene QUIIF to actual rocks are given in the companion paper (Frost and Lindsley, 1992). In this section we describe some general principles regarding the use of calcium pyroxene QUIIF. In the ideal world, oxides would retain

their high-temperature compositions through cooling, and the happy petrologist could obtain the maximum amount of information from a given mineral assemblage as outlined in the previous discussion. In the imperfect real world, however, oxides are very prone to resetting, such that even in volcanic rocks one must be concerned with whether the temperature and f_{O_2} they record are actually those of the original magma chamber. If there are enough phases in the assemblage, one can evaluate the intensive parameters, even if some reequilibration has occurred. In studying dozens of examples, we have found only one for which the oxide temperatures are greater than the pyroxene temperatures, but many for which the reverse is true. Thus in the examples below, it is the oxides that are assumed to have reset.

Assemblages with two oxides, two pyroxenes, and olivine or quartz. For example, in assemblages with two pyroxenes, two oxides, and either olivine or quartz (OpAUIIO, OpPUIIO, APUIIO; or QUIIOpA, QUIIAP, QUIIOpP) or the assemblage fayalite + quartz + hedenbergite + two oxides (QUIIOA), a reasonable estimate of equilibration conditions can be made even if the oxides have reset. One way to visualize this is shown in Figure 5. The pyroxenes should record a temperature, or rather a temperature range (shown as T_{Px} in Figs. 5A–5C), corresponding to analytical uncertainty in the compositions. The oxides from this rock will also indicate values of T and f_{O_2}. As with the pyroxenes, uncertainties in composition of the oxides will yield ranges of T and f_{O_2}, which will generally outline a diamond-shaped region of acceptable values. If this diamond falls within, or at least partially overlaps, the band of pyroxene temperatures (Fig. 5A), it is very likely that the region of overlap includes the temperature and f_{O_2} at which the oxides and pyroxenes had been in equilibrium. That conclusion would be strengthened if it were found that the oxides were also in Fe-Mg exchange with the silicates. We have found, however, that oxides exchange Fe and Mg much more readily than they exchange Ti and Fe^{3+}, so the lack of Fe-Mg exchange equilibrium between the silicates and oxides does not necessarily indicate overall disequilibrium (Frost and Lindsley, 1992).

The process outlined so far simply has used two independent thermometers to find a temperature of mutual equilibrium. But QUIIF permits us to do more. If the olivine is in Fe-Mg exchange equilibrium with the pyroxenes, which is easily verified with the QUILF computer program, we can calculate the equilibrium f_{O_2} for the assemblage OpAUIIO. Because the f_{O_2} of OpAUIIO moves to lower values with increasing pressures, we can find a pressure range (approximately P_2 to P_4 in Fig. 5A) for which the OpUIIO f_{O_2} will be consistent with the equilibrium T and f_{O_2} as defined by the oxides and pyroxenes. Furthermore, if pressure is known to fall in a narrower range (say between P_3 and P_4 in Fig. 5A), the possible range of f_{O_2} is reduced. (If we had used the quartz-saturated assemblage QUIIOpA, the relation between pressure and f_{O_2} would be reversed.) In addition, although not shown on Figure 5A, the silica activity of this assemblage can also be determined by the displacement of the FMQ buffer to the appropriate T and f_{O_2}.

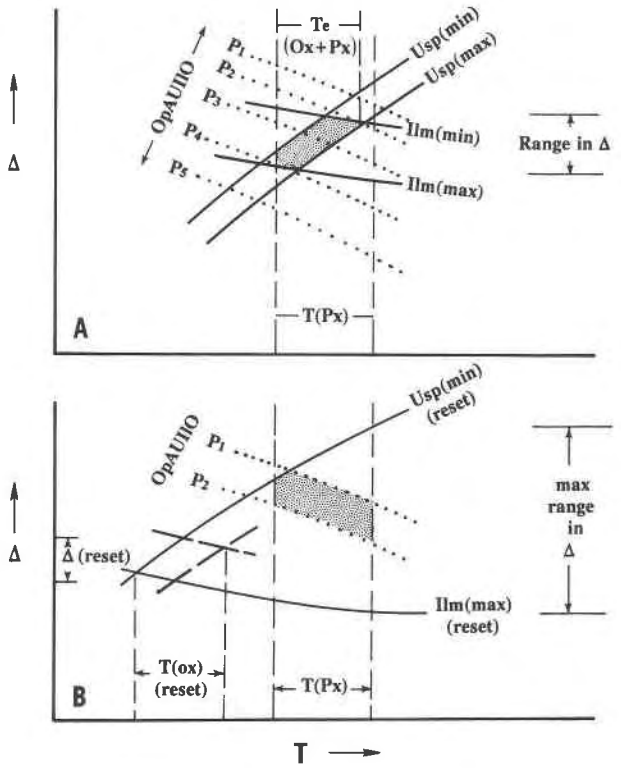

Fig. 5. Schematic diagrams of T vs. $\Delta \log f_{O_2}$ illustrating the use of calcium pyroxene QUIIF equilibria to constrain intensive parameters for the assemblage 2 pyroxenes + 2 oxides + olivine. Lines labeled Usp and Ilm are lines of constant N_{Ti} in titaniferous magnetite and of constant $X_{il} + X_{gk}$ in ilmenite (N_{Mn} and X_{py} are assumed to be zero). (**A**) Case for which the oxides and pyroxenes give identical temperature ranges, within analytical uncertainty. Oxygen fugacities calculated for the OpAUIIO (or APUIIO) assemblage (dotted lines) agree with f_{O_2} from the oxides only at pressures from P_2 to P_4 and thus constrain the pressure to that range, if all phases were in equilibrium. (**B**) Case for which one or both oxides has reset composition to temperatures below that of initial equilibrium with the pyroxenes. If resetting of the oxides took place in a closed system, the initial f_{O_2} is constrained to have been in the area below the Usp isopleth and above the Ilm isopleth. If pressure is known independently (for example, it is known to fall between P_1 and P_2), then initial f_{O_2} can be further constrained by QUIIOpA to lie within the stippled region.

Now suppose that the oxides had initially been in equilibrium with the silicates but subsequently changed their compositions by inter-oxide exchange during cooling. In this case, the temperature and f_{O_2} defined by the oxides would not overlap the band of pyroxene temperatures (Fig. 5B), but would outline a diamond at lower temperatures. (This geometry could also form if the oxides had simply crystallized later and at a lower temperature than the pyroxenes, so it is the responsibility of the petrologist

to adduce textural or other evidence that the oxides and pyroxenes had originally been in equilibrium.) If the oxides had cooled in a closed system, then their compositional changes can be modeled (Frost et al., 1988, their Fig. 4). If the dominant oxide were magnetite, its composition would remain relatively unchanged during reequilibration, and the cooling would have followed an ulvöspinel isopleth. Conversely, if ilmenite were dominant, the cooling path would have followed an ilmenite isopleth. Put another way, upon equilibrium cooling in a closed system, ilmenite gains $FeTiO_3$ and titaniferous magnetite gains Fe_3O_4. Therefore the primary ilmenite is not likely to have been richer in Fe^{3+} nor the titaniferous magnetite to have been poorer in Ti than the analyzed values. It is thus probable that the original f_{O_2} fell on or below that of the ulvöspinel isopleth, and on or above that of the ilmenite isopleth within the band of pyroxene temperatures (Fig. 5B). If the relative abundances of the oxides are known, then we can calculate a relatively narrow cooling path within this band. If the abundances are unknown, however, the best we can do is to evaluate equilibrium within the possible range of f_{O_2}. The range in f_{O_2}, pressures, and silica activities at which this assemblage formed can therefore be obtained as follows. The maximum f_{O_2} (and minimum pressure) can be obtained by determining the f_{O_2} at which a titaniferous magnetite of the given composition is in equilibrium with some ilmenite of unspecified composition over the range of pyroxene temperatures. Likewise, the minimum f_{O_2} (and maximum pressure) is obtained by determining the f_{O_2} at which an ilmenite of the given composition is in equilibrium with titaniferous magnetite of unspecified composition. These constraints outline the shaded area in Figure 5B. In the discussion above, the terms ulvöspinel isopleth and ilmenite isopleth are holdovers from the days of treating the oxides as binary phases (e.g., Frost et al., 1988). In pyroxene QUIIF we explicitly consider Mg components in the oxides. For this case, ulvöspinel should be taken to mean $(Fe,Mg)_2TiO_4$ (or N_{Ti}) and ilmenite to mean $X_{il} + X_{gk}$ (or $1 - X_{hem}$).

The technique described above may work well if the oxides have reacted to temperatures only slightly below that of the silicates. If the equilibration is extreme, however, as is common in plutonic rocks, the range of possible pressures and f_{O_2} for the assemblage may become ludicrously large. If one oxide is modally dominant, the crystallization conditions are likely to be close to the isopleth for that phase. If neither is dominant or the modal proportions are unknown, one may have to assume a reasonable range in pressure in order to estimate reasonable values for f_{O_2} and silica activity (ruled area in Fig. 5B).

Assemblages with two pyroxenes and two oxides. Theoretically one can obtain nearly the same information from four-phase assemblages with two pyroxenes and two oxides as was obtained with the five-phase assemblage described above. Such divariant assemblages must fall between the QUIIOpA and OpAUIIO curves—or the equivalent reactions containing pigeonite. If the oxides were in equilibrium with the silicates, then one can get temperature from the oxides and pyroxenes, f_{O_2} from the oxides, silica activity from the displaced OpAMQ equilibrium, and pressure from the displaced QUIIOpA equilibrium. However, pressure and silica activity calculated by this method are poorly constrained; even a small variation in T or f_{O_2} will produce large variations in pressure and silica activity. The values of these parameters vary together, so that if one can be fixed independently, the other will be closely limited.

If the oxides are no longer in equilibrium with the pyroxenes, the best way to treat this assemblage is to estimate a range of possible pressures and to calculate the range of f_{O_2} over which the assemblage can occur for each pressure. Even if one knows nothing about the oxide compositions nor whether the oxides have undergone resetting, the assemblage two pyroxenes + two oxides is limited at high f_{O_2} by the reaction of ilmenite with low-Ca pyroxene to make titaniferous magnetite + high-Ca pyroxene + quartz (Reactions 12, QUIIOpA; 19, QUIIAP; or 20, QUIIOpP) and at low f_{O_2} by the reaction of titaniferous magnetite + low-Ca pyroxene to make higher Ca pyroxene + olivine + ilmenite (Reaction 13, OpAUIIO; 21, OpPUIIO; or 22, APUIIO). This idea is illustrated for pigeonite-free reactions in Figure 6A, where the f_{O_2} must lie between Reaction 12, QUIIOpA, and 13, OpAUIIO. If the oxides have not cooled far from their original compositions, then one may be able to limit the f_{O_2} further by using the Usp and Ilm isopleths, as described above and also shown in Figure 6A.

For some samples, particularly those that formed at relatively high silica activities or which have ilmenite as the major oxide, the projected ulvöspinel isopleth will lie above the QUIIOpA surface (Fig. 6B). In this situation, the QUIIOpA assemblage (i.e., quartz saturation) will provide the upper limit on f_{O_2} whereas the lower will be the ilmenite isopleth. For other samples, most likely those that formed at relatively low silica activities or have magnetite as the major oxide, the projected ilmenite isopleth would lie at f_{O_2} below those of the OpAUIIO assemblage (Fig. 6C). In this case, the OpAUIIO surface would form the lower limit, and the Usp isopleth would mark the upper limit for f_{O_2}.

The assemblage Opx + Q + Mt + Ilm

A common assemblage in rhyolites is Opx + quartz + two oxides, without coexisting clinopyroxene. If the two oxides retain equilibrium with the Opx, this assemblage can be used to give temperature, pressure, and f_{O_2}. However, if the oxides have reset, one can still obtain a range of T and f_{O_2} for this assemblage by assuming a pressure or a range in pressures and calculating the equilibrium T and f_{O_2} for constant titaniferous magnetite composition (letting the ilmenite composition float) and for constant ilmenite composition (letting the titaniferous magnetite composition float). In Figure 7 this is shown schemati-

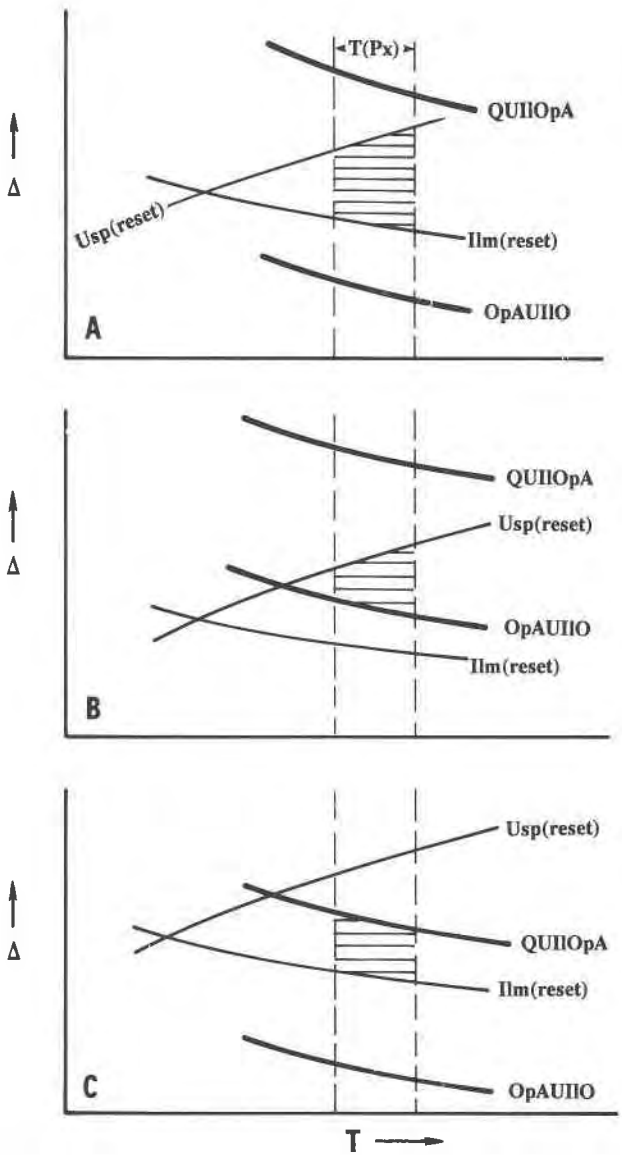

Fig. 6. Schematic diagrams of T vs. $\Delta \log f_{O_2}$ illustrating the use of calcium pyroxene QUIIF equilibria to constrain intensive parameters for the assemblage 2 pyroxenes + 2 oxides, without either olivine or quartz. Labels as in Figure 5. For clarity, only the minimum Usp (reset) and maximum Ilm (reset) isopleths are shown. (**A**) Oxide compositions are unknown or have been reset to lower temperatures. The f_{O_2} must lie below QUIIOpA (otherwise quartz would be present) but above OpAUIIO (or olivine would be present). If oxide compositions are known, the f_{O_2} may be further constrained to lie between the (reset) Usp and Ilm isopleths (hatched area). (**B**) Case for which the QUIIOpA curve rather than the Usp isopleth sets upper limit on f_{O_2}. (**C**) Case for which the OpAUIIO curve rather than the Ilm isopleth sets lower limit on f_{O_2}.

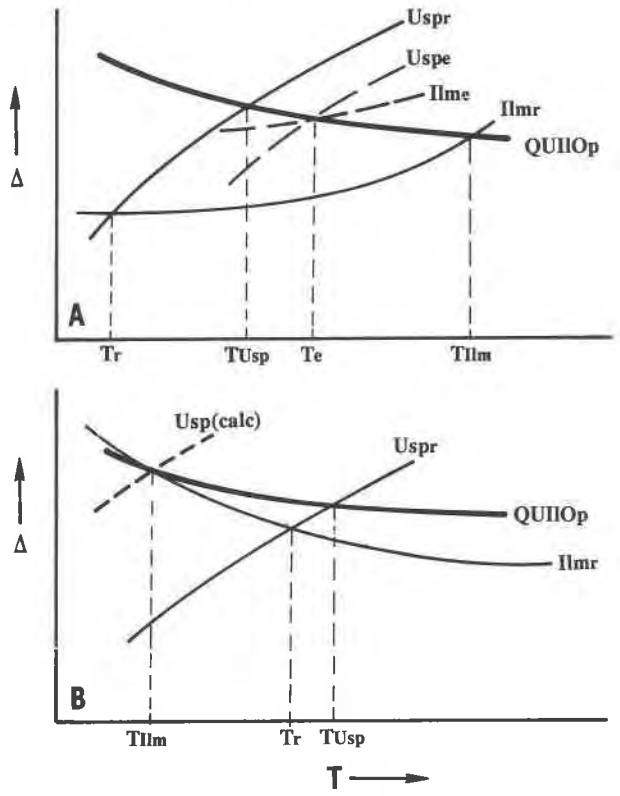

Fig. 7. Schematic diagrams of T vs. $\Delta \log f_{O_2}$ outlining the method for estimating temperature and f_{O_2} for assemblages of two oxides + Opx + quartz. For clarity, isopleths are shown without associated errors. (**A**) If the oxides have not reset, their equilibrium isopleths (Usp_e and Ilm_e) should intersect with the QUIIOp curve at the equilibrium temperature (T_e) and f_{O_2}. If the oxides have reset, the original temperature and f_{O_2} must have lain on the segment of QUIIOp that falls between the Usp_r ($<Usp_e$) and Ilm_r ($>Ilm_e$) isopleths. (**B**) Special case for low temperatures at which Ilm isopleths curve sharply upward with decreasing T. The reset ilmenite isopleth (Ilm_r) may intersect the QUIIOp curve at a temperature well below that indicated by the spinel isopleth (Usp_r). Note that the spinel isopleth (Usp_{calc}) suggested by the ilmenite is much lower in Ti than the observed composition (Usp_r). If the temperature indicated by the reset ilmenite were the true equilibrium temperature, the coexisting spinel would have had to gain Ti upon cooling—a most implausible result. Therefore we know only that $T_e > T_{Usp}$.

cally by the intersection of the QUIIOp curve with the Usp and Ilm isopleths.

For many high-temperature rhyolites the temperature calculated at constant X_{Usp} will lie below that calculated at constant X_{Ilm} (Fig. 7A), and the equilibrium T and f_{O_2} must lie along QUIIOp between the two. For some low-temperature conditions, however, where the ilmenite isopleths have a steep negative slope (Fig. 3 of Andersen and Lindsley, 1988), the temperature (T_{Ilm_r}) deduced from the intersection of the reset Ilm isopleth with QUIIOp will lie below that deduced from the reset Usp isopleth (T_{Usp_r}) (Fig. 7B). In such an instance T_{Ilm_r} has no meaning because the calculated titaniferous magnetite (Usp_{calc}) would be poorer in Ti than the analyzed titaniferous magnetite (Usp_r). Since it is most unlikely that titaniferous magnetite can gain Ti on cooling, T_{Ilm_r} can have nothing to do with the equilibrium conditions of the oxides and

the silicates. Rather the equilibrium conditions must lie at higher T and lower f_{O_2} than the intersection of the Usp isopleth with the QUIIOp surface. In this situation, unfortunately, there is no way of determining the maximum T or minimum f_{O_2}.

The assemblage two pyroxenes + magnetite

The assemblage of two pyroxenes and magnetite without ilmenite is common in andesitic and some dacitic rocks. In some andesites, olivine may be present also, but for very few is it in equilibrium with the pyroxenes. If olivine is present and in equilibrium, then one can calculate T and f_{O_2}, if pressure is known or can be estimated. If olivine is lacking or not in equilibrium, however, one can still calculate the range of f_{O_2} over which this assemblage could occur. Since there is no phase with which to exchange Ti, the titaniferous magnetite analyzed in this assemblage is likely to represent the equilibrium composition. The lower limit of f_{O_2} would therefore be olivine saturation, i.e., the f_{O_2} at which low-Ca pyroxene + titaniferous magnetite would react to pyroxene richer in Ca + olivine + ilmenite (OpAUIIO, OpPUIIO, or APUIIO). The high f_{O_2} limits would be those at which titaniferous magnetite of the observed composition would react to produce ilmenite (i.e., an ulvöspinel isopleth).

These are only a few examples of the ways in which the calcium pyroxene QUIIF can be used to set limits on intensive parameters even when the oxides have reset. There are so many assemblages possible among oxides, pyroxenes, olivine, and quartz that it is not practical to present the strategies used for each. These examples show how the reasoning works, and it should be relatively easy for the reader to apply the methods to other assemblages.

Summary and conclusions

Calcium pyroxene QUIIF is an extensive series of reactions and equilibria that relate oxides, pyroxenes, olivine, and quartz for compositions that plot in or close to the system Fe-O-CaO-MgO-TiO_2-SiO_2. Because all phases except quartz are solid solutions, intensive parameters of crystallization can be determined even for assemblages of relatively high variance in a phase-rule sense. Five-phase assemblages, which have a formal variance of three, will generally yield quantitative values of T, P, f_{O_2}, and a_{SiO_2}; in favorable circumstances those parameters can be extracted from four-phase assemblages as well. A computer program, QUILF, is available to perform the calculations (Andersen et al., in preparation). The method is applied to a variety of igneous rocks in the following paper (Frost and Lindsley, 1992).

Obtaining working copies of the QUILF program

QUILF is written in Turbo Pascal for IBM PC and compatible computers. Programs to project compositions are also available. Readers who wish to obtain copies of program QUILF and the projection programs should send an unformatted diskette (3.5 or 5.25 in.; 360 K is adequate) and a separate self-addressed adhesive mailing label to D.H.L. It has been our experience that approximately one in ten diskettes becomes physically (not magnetically) damaged in the mails; accordingly, readers should be sure that their diskettes are well protected, preferably in sturdy mailers. Because of previous bad experiences of users modifying our programs and then announcing publicly that our programs were flawed, we prefer to supply compiled programs only. Readers who request the source codes should send two diskettes and a convincing statement as to why they require the source codes. The projection programs require IBM Basic (or GWBASIC); we supply them in ASCII format so that they may be imported into other versions of Basic, but it is the user's responsibility to make any changes necessary to render them compatible with those versions.

Acknowledgments

We are grateful to David Andersen and Paula Davidson for doing most of the development of the solution models and are especially indebted to D.J. Andersen for producing the QUILF program in a convenient form. We thank John Haas for providing his unpublished compilation of Fe-O-SiO_2-O_2 buffers. The presentation has been significantly improved through diligent and perceptive reviews by Rob Berman and Mark Ghiorso, and we are deeply grateful to them. This work has been supported by NSF grants EAR-8720185 and EAR-8816040 to D.H.L. and EAR-8816604 to B.R.F., which we gratefully acknowledge. D.H.L. thanks the Department of Geology and Geophysics at the University of Wyoming for its support and hospitality during the fall semester, 1990, when most of this paper was written. Stony Brook Mineral Physics Insitute publication no. 62.

References cited

Andersen, D.J., and Lindsley, D.H. (1988) Internally consistent solution models for Fe-Mg-Mn-Ti oxides: Fe-Ti oxides. American Mineralogist, 73, 714–726.

Andersen, D.J., Bishop, F.C., and Lindsley, D.H. (1991) Internally consistent solution models for Fe-Mg-Mn-Ti oxides: Fe-Mg-Ti oxides and olivine. American Mineralogist, 76, 427–444.

Bohlen, S.R., Essene, E.J., and Boettcher, A.L. (1980) Reinvestigation and application of olivine-quartz-Opx barometry. Earth and Planetary Science Letters, 47, 1–10.

Bowen, N.L., and Schairer, J.F. (1935) The system MgO-FeO-SiO_2. American Journal of Science, 29, 151–217.

Buddington, A.F., and Lindsley, D.H. (1964) Iron-titanium oxide minerals and synthetic equivalents. Journal of Petrology, 5, 310–357.

Carmichael, I.S.E. (1967a) The iron-titanium oxides of salic volcanic rocks and their associated ferromagnesian silicates. Contributions to Mineralogy and Petrology, 14, 36–64.

——— (1967b) The mineralogy of Thingmuli, a Tertiary volcano in eastern Iceland. American Mineralogist, 52, 1815–1841.

Davidson, P.M., and Lindsley, D.H. (1989) Thermodynamic analysis of pyroxene-olivine-quartz equilibria in the system CaO-MgO-FeO-SiO_2. American Mineralogist, 74, 18–30.

Davidson, P.M., and Mukhopadhyay, D.K. (1984) Ca-Fe-Mg olivines: Phase relations and a solution model. Contributions to Mineralogy and Petrology, 86, 256–263.

Frost, B.R., and Lindsley, D.H. (1992) Equilibria among Fe-Ti oxides, pyroxenes, olivine, and quartz: Part II. Application. American Mineralogist, 77, 1004–1020.

Frost, B.R., Lindsley, D.H., and Andersen, D.J. (1988) Fe-Ti oxide-silicate equilibria: Assemblages with fayalitic olivine. American Mineralogist, 73, 727–740.

Ghiorso, M.S., and Sack, R.O. (1989) A reappraisal of Fe-Ti oxide geothermometry in light of new thermodynamic solution models for Mg-Fe^{2+}-Al-Fe^{3+}-Ti spinel and Mg-Fe^{2+}-Fe^{3+} rhombohedral oxide solid solutions. Eos, 70, 1387.

——— (1991) Fe-Ti oxide geothermometry: Thermodynamic formulation and the estimation of intensive variables in silicic magmas. Contributions to Mineralogy and Petrology, 108, 485–510.

Helgeson, H.C., Delany, J.M., Nesbit, H.W., and Bird, D.K. (1978) Summary and critique of the thermodynamic properties of rock-forming minerals. American Journal of Science, 278A, 1–229.

Johnston, A.D., and Stout, J.H. (1984) A highly oxidized ferroan salite-, kennedyite-, forsterite-, and rhonite-bearing alkali gabbro from Kawai, Hawaii, and its mantle xenoliths. American Mineralogist, 69, 57–68.

Lindsley, D.H., Frost, B.R., Andersen, D.J., and Davidson, P.M. (1990) Fe-Ti oxide–silicate equilibria: Assemblages with orthopyroxene. In R.J. Spencer and I.-M. Chou, Eds., Fluid-mineral interactions: A tribute to H.P. Eugster, Special Publication 2, p. 103–119. The Geochemical Society, San Antonio, Texas.

Osborn, E.F. (1959) Role of oxygen pressure in the crystallization and differentiation of basaltic magma. American Journal of Science, 257, 609–647.

Robie, R.A., Finch, C.B, and Hemingway, B.S. (1982) Heat capacity and entropy of fayalite (Fe_2SiO_4) between 5.1 and 383 K: Comparison of calorimetric and equilibrium values for the QFM buffer reaction. American Mineralogist, 67, 463–469.

Manuscript received February 12, 1991
Manuscript accepted May 4, 1992